Real-Time Modal Analysis of Electric Power Grids–The Need for Dynamic State Estimation

Preprint

Marcos Netto,[1] Venkat Krishnan,[1] Lamine Mili,[2]
Pranav Sharma[3] and Venkataramana Ajjarapu[3]

[1] *National Renewable Energy Laboratory*
[2] *Virginia Polytechnic Institute and State University*
[3] *Iowa State University*

Real-Time Modal Analysis of Electric Power Grids–The Need for Dynamic State Estimation
Preprint

Marcos Netto,[1] Venkat Krishnan,[1] Lamine Mili,[2]
Pranav Sharma[3] and Venkataramana Ajjarapu[3]

[1] *National Renewable Energy Laboratory*
[2] *Virginia Polytechnic Institute and State University*
[3] *Iowa State University*

Suggested Citation

NOTICE

Real-Time Modal Analysis of Electric Power Grids– The Need for Dynamic State Estimation

Marcos Netto, *Member, IEEE,* Venkat Krishnan, *Senior Member, IEEE,* Lamine Mili, *Life Fellow, IEEE,* Pranav Sharma, *Student Member, IEEE,* Venkataramana Ajjarapu, *Fellow, IEEE*

Abstract—We articulate the reason why dynamic state estimation is needed to push the boundaries of the modal analysis of electric power grids in real-time operation. Then, we demonstrate how to unravel linear and nonlinear modes by using the extended dynamic mode decomposition along with estimates of the synchronous generators' rotor angles and rotor speed deviations from nominal speed. The estimated modes are associated with electromechanical oscillations that take place continuously in electric power grids because of imbalances between power generation and demand. The numerical simulations are performed on a synthetic, albeit realistic, 2,000-bus network that was designed to resemble the electric power grid of Texas.

Index Terms—Dynamic state estimation, extended dynamic mode decomposition, Koopman operator, modal analysis.

I. INTRODUCTION

Modal analysis of electric power grids based on system models is a suitable approach for planning studies [1]. Conversely, data-driven methods are preferred for real-time operation [2], [3]. Data-driven modal analysis methods are classified based on the type of data—*ambient* [4], *probing* [5] or *ringdown* [6]—they are suitable for [7]. The basic assumption for ambient data is that the system is in a quasi-steady-state condition, slightly perturbed by random variations in power demand. Conversely, ringdown data arise following major disturbances, in which case the system states experience large excursions. Probing data stems from an intrusive approach—that is, signals are injected into the grid to aid in revealing otherwise hidden information. The current practice in real-time operation is to rely on either ambient or probing signals to monitor the system modes. If an excited mode is underdamped, then a corrective measure is taken by the system operator. Note that this philosophy of design "is that of preventive control, i.e., changing system operating conditions before a fault happens to ensure the system can withstand the fault" [8]. Preventive control is important in real-time operation; however, our interest is in designing modal control schemes that will automatically steer the system after an unforeseen fault happens. Timing is mission critical under these circumstances, and hence automatic control is necessary. For this reason, we focus exclusively on ringdown signals.

Our investigation is motivated by the fact that synchrophasor measurements of bus voltage angle (or frequency) have been used as a proxy for synchronous generators' rotor angle (or speed) [9]; this is done because measurements of synchronous generators' rotor angle and speed are not available [10]. However, using synchrophasor measurements as a proxy for dynamic state variables might lead to poor estimation of the system modes. One reason for this lies in the discontinuities caused by, e.g., switching or short-circuit, which occur on the quantities measured by phasor measurement units (PMUs). These quantities are represented by algebraic variables within the set of differential-algebraic equations that model the power grid, wherein the continuous differential equations dictate the actual dynamic states of the system. Discontinuities alter the spectrum of the signal. This is well-known in signal processing [11] and carefully addressed by the dynamical systems community. See, for instance, [12], where it is assumed that the space of observable functions is $\mathcal{F} \subseteq C^0$, and C^0 denotes all continuous functions. Along the same lines, the synchronous generators' rotor angle and speed are continuous quantities, i.e., they are not allowed by the laws of physics to vary instantly.

This paper addresses this problem by using synchrophasor measurements, along with models of the synchronous generators, to estimate the dynamic state variables. Therefore, a real-time modal analysis that can use the state estimates of rotor angle (or speed) is ideal, rather than analysis that uses direct measurements of bus voltage angle (or frequency). To the authors' knowledge, this is the first attempt to use dynamic state estimation to aid in real-time modal analysis of electric power grids. We proceed further on the use case of real-time modal analysis aided by dynamic state estimation (DSE). Specifically, we study the effectiveness of extended dynamic mode decomposition (EDMD) [13], [14] in uncovering linear and nonlinear modes from estimates of the synchronous generators' rotor angle and speed, which are obtained from DSE. We aim to assess the benefits of relying on EDMD to carry out modal analysis of electric power grids in real time. Last, note that it is common for the terms *modal analysis* and *small-signal stability analysis* to be used interchangeably in power system literature. This is not the case in this paper. The modal analysis approach we adopt is based on the Koopman operator-theoretic framework [15]. The stability inferred from the spectrum of the Koopman operator is valid for the entire domain of attraction [16], and it provides a global, rather than a local, measure of stability.

The paper proceeds as follows. Section II introduces the concept of linear and nonlinear modes. The DSE-aided modal analysis of a realistic power grid is performed and analyzed in Section III. Conclusions are given in Section IV.

II. PRELIMINARIES

Consider the nonlinear dynamical system $\dot{\boldsymbol{x}}(t) = \boldsymbol{f}(\boldsymbol{x}(t))$, where $\boldsymbol{x}(t) \in \mathbb{R}^n$ is the state vector, and $\boldsymbol{f} : \mathbb{R}^n \to \mathbb{R}^n$ is a smooth vector field satisfying $\boldsymbol{f}(\boldsymbol{0}) = \boldsymbol{0}$. We can formally construct the Taylor expansion of $\boldsymbol{f}$ about $\boldsymbol{0}$:

$$\dot{\boldsymbol{x}} = \boldsymbol{A}\boldsymbol{x} + \boldsymbol{X}_2 + ... + \boldsymbol{X}_k + \mathcal{O}(|\boldsymbol{x}|^{k+1}), \qquad (1)$$

where $\boldsymbol{X}_p \in H^p$, the real vector space of vector fields whose components are homogeneous polynomials of degree p. If we neglect second- and higher order nonlinear terms in (1), then:

$$\dot{\boldsymbol{x}} = \boldsymbol{A}\boldsymbol{x}. \qquad (2)$$

Now, assume that the matrix $\boldsymbol{A}$ has n distinct eigenvalues $(\lambda_1, ..., \lambda_n)$. Let $\boldsymbol{r}_i$ be the i-th right eigenvector of matrix $\boldsymbol{A}$. Let $\boldsymbol{\ell}_i$ denote the i-th left (row) eigenvector of matrix $\boldsymbol{A}$. The solution of (2) is given by a sum of modal components, or *linear modes*:

$$\boldsymbol{x} = \sum_{i=1}^{n} e^{\lambda_i t} \boldsymbol{c}_i, \qquad (3)$$

where $\boldsymbol{c}_i$ are constant vectors defined by the initial state vector $\boldsymbol{x}(0) = \boldsymbol{x}_0$, and by the eigenvectors $\boldsymbol{r}_i$ and $\boldsymbol{\ell}_i$.

Definition 1. *The i-th linear mode is given by:* $e^{\lambda_i t} (\boldsymbol{\ell}_i \boldsymbol{x}_0) \boldsymbol{r}_i$.

The definition of nonlinear modes adopted in electric power grids relies on the normal forms for vector fields [17]. If the third- and higher order terms in (1) are neglected, then:

$$\dot{\boldsymbol{x}} = \boldsymbol{A}\boldsymbol{x} + \boldsymbol{X}_2. \qquad (4)$$

It was shown in [18] that the solution of (4) is given by:

$$\boldsymbol{x} = \sum_{i=1}^{n} e^{\lambda_i t} \boldsymbol{c}_i + \sum_{i=1}^{n} \boldsymbol{r}_i \left[\sum_{j=1}^{n} \sum_{k=1}^{n} e^{(\lambda_j + \lambda_k)t} \boldsymbol{d}_i \right], \qquad (5)$$

where $\boldsymbol{d}_i$ are vectors obtained from $\boldsymbol{x}_0$, $\boldsymbol{r}$, $\boldsymbol{\ell}$ and a sequence of coordinate transformations that are executed in the process of putting (4) in its normal form. See [19] and references therein for more details. The rightmost sum of the modal components in (5) defines the *second-order nonlinear modes*. Recently, third-order nonlinear modes have also been considered [20].

Definition 2. *The damping ratio, ξ, of the i-th linear mode is defined as:*

$$\xi_i := -\frac{\mathcal{R}e(\lambda_i)}{|\lambda_i|} = -\frac{\sigma_i}{\sqrt{\sigma_i^2 + \omega_i^2}}. \qquad (6)$$

Proposition 1. *In a stable system, the damping ratio of any second-order nonlinear mode is larger than or equal to the smallest damping ratio among all linear modes.*

Proof. It is straightforward to verify this result geometrically; see Fig. 1. □
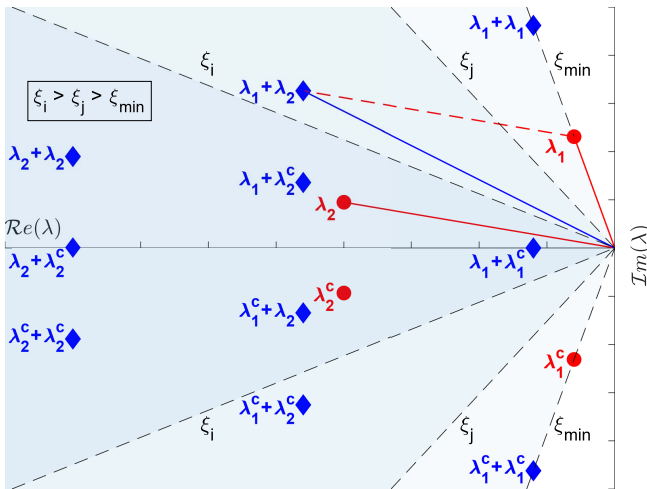

Fig. 1. Geometric picture of Proposition 1.

Proposition 1 implies that if the damping ratio of all linear modes is adequate—that is, it is larger than a predefined

threshold—then so is the damping ratio of the nonlinear modes. Hence, it might be enough to rely exclusively on linear modes if the objective is to ensure that electromechanical oscillations will be sufficiently damped. The damping ratio provides a certain measure of stability margin and is informative for preventive control actions. If a disturbance takes the system far from the equilibrium point, however, then it is necessary to forecast the trajectory before taking automatic control actions to steer the system to a safe operating region. In this case, the linear modes only provide an incomplete picture, and thus nonlinear modes are required. This is promptly realized by comparing (3) to (5), and it has motivated recent investigations; see, e.g., [21], [22]. Example 1 is used to further demonstrate this fact about the importance of nonlinear modes.

Example 1. *Single-machine infinite-bus system.*
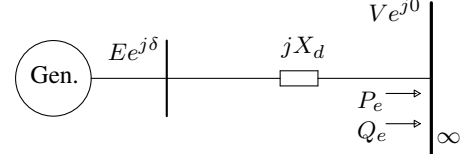
Fig. 2. One-line diagram of single-machine infinite bus system.

The system in Fig. 2 is mathematically represented by:

$$\dot{\delta}_i = \omega_i, \qquad (7)$$

$$M\dot{\omega}_i = 0.9 - \frac{EV}{X_d} \sin(\delta - \delta_{sep}), \qquad (8)$$

where $P_e = 100$ MVA, $Q_e = 50$ MVA, $S_{base} = 100$ MVA, $f_{base} = 60$ Hz, $V = 1.05$ per unit, $M = 5/60\pi$ seconds, and $X_d = 1.2$ per unit. Note that the stable equilibrium point is shifted to the origin and $\delta_{sep} = 0.545$ radians. This system has a pair of complex-conjugate eigenvalues: $\lambda_{1,2} = \pm j7.4801$.

Now, suppose that $\boldsymbol{x}_0 = (1.5, 1.5)$. Fig. 3 shows that the forecast of the state trajectory using exclusively linear modes is poor, and the inclusion of nonlinear modes enhances the forecasting. Therefore, the modal analysis discussed in the rest of this paper will include both linear and nonlinear modes.
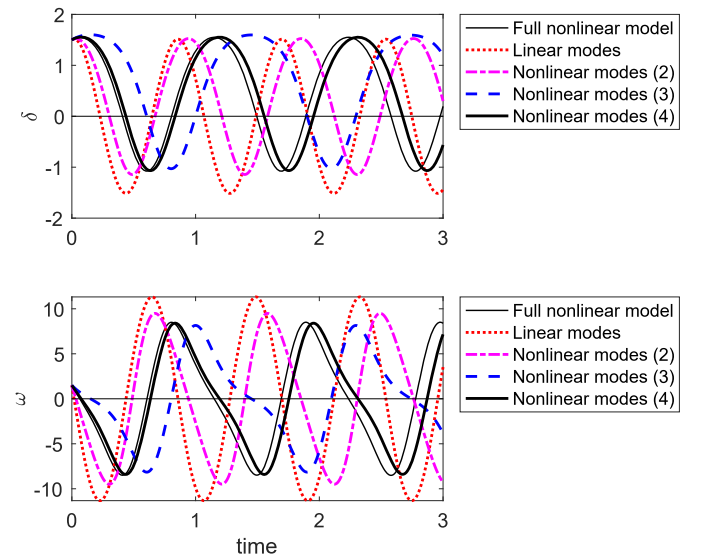
Fig. 3. State trajectory starting at $\boldsymbol{x}_0 = (1.5, 1.5)$. In the legend, 'Nonlinear modes (2)' indicates that linear and second-order nonlinear modes are used to perform the forecasting. Likewise, 'Nonlinear modes (3)' indicates that linear, second-, and third-order nonlinear modes are used to perform the forecasting.

2

TABLE I
TABLE I
DESCRIPTION OF THE GENERATORS.

Number	Type	Installed Capacity	Model	Controls
87	Wind	15,089 MVA	WT4G1	WT4E1
457	Synchronous	102,405 MVA	GENROU and GENSAL.	Turbine-governor, excitation, and stabilizer.

III. DATA-DRIVEN MODAL ANALYSIS OF A LARGE ELECTRIC POWER GRID

The results in this section are obtained by numerical simulations of the 2,000-bus network that resembles the footprint of the Texas power grid[1]. This synthetic model has been developed under the Generating Realistic Information for Development of Distribution And Transmission Algorithms (GRID DATA) program[2], sponsored by Advanced Research Projects Agency-Energy (ARPA-E). This model has been validated to respond like a real power grid [23]. Table I summarizes the generator's models in the base case. Note that the WT4G1 model is adopted for all wind machines; this implies that they are equipped with full back-to-back converters and do not contribute to the electromechanical oscillations. All the synchronous machines are modeled with turbine-governor and excitation systems, as well as power system stabilizers, of various degrees of complexity. The final system model has 6,147 state variables.

A total of 6,147 linear modes is obtained by small-signal analysis of the base case. The eigenvalues associated with these linear modes are plotted in the complex plane in Fig. 4a. Of those, Table II presents the ones with a damping ratio smaller than 10%. Our interest is in the reduced frequency range shown in Fig. 4b, which spans most electromechanical phenomena. A subset of the eigenvalues associated with second-order nonlinear modes [19] is computed based on the eigenvalues in Table II. For example, the eigenvalue:

$$\lambda_{215} + \lambda_{260} = (-0.391 + j11.885) + (-0.502 + j12.294)$$

is associated with a second-order nonlinear mode of frequency 3.848 Hz. Recall that all complex eigenvalues appear in complex conjugate pairs because the Jacobian matrix is real-valued. Hence, there are 116 complex-conjugate eigenvalues associated with the 58 linear modes in Table II. From the combination of 116 two-by-two, 6,670 eigenvalues associated with second-order nonlinear modes are calculated. They are also shown in Figs. 4a and 4b.
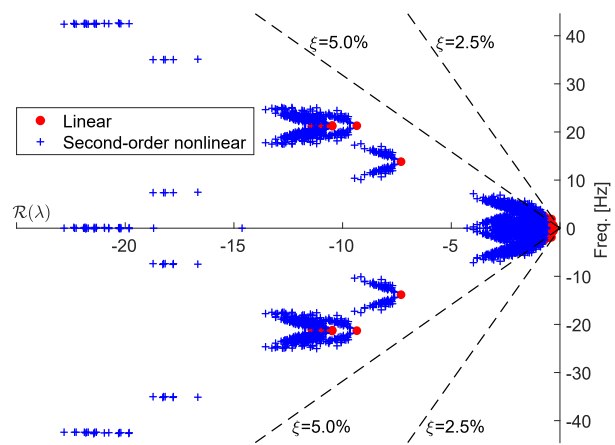
A. Synthetic Measurements

In the system described in the previous section, a three-phase short-circuit is applied at Bus 6031 and cleared after 10 ms. This event is designed to excite the linear mode 215 shown in Table II. Note that the type, location, and duration of the fault will affect the extent by which modes are excited. Different events will lead to modes being excited differently. Nonetheless, the conclusions presented here will remain valid. The rationale of the design can be explained as follows:

- Mode-in-state participation factors [24] are computed.
- The linear mode 215 has a participation factor of 1.00 in the state variables associated with the synchronous generator connected to Bus 6272, i.e., mode 215 is strongly affected by the generator connected to Bus 6272.
- The short-circuit is applied at Bus 6031 because it is the closest, in the sense of electrical distance, to Bus 6272.

The event is simulated in PSS/E software and time-series data are recorded for 10 s after the fault is cleared. An additive random

[1] Available at https://electricgrids.engr.tamu.edu/electric-grid-test-cases/.
[2] For more details, https://arpa-e.energy.gov/?q=arpa-e-programs/grid-data.

(a) All computed eigenvalues.
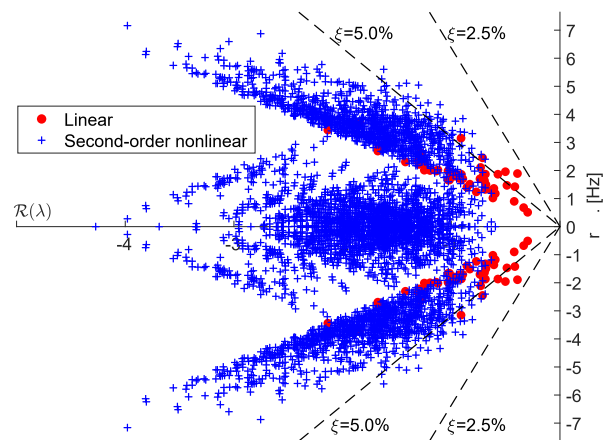
(b) Eigenvalues in the frequency range of interest.

Fig. 4. Eigenvalues associated with linear and second-order nonlinear modes.

Gaussian noise with zero mean and standard deviation $\sigma = 10^{-2}$ is assumed for each of the following:

- Synchronous generator real (P) and reactive (Q) power;
- Bus voltage magnitude (V), phase angle (θ), and frequency deviation from nominal (f).

B. Dynamic State Estimation

Many DSE algorithms conceived in a centralized [25]–[30], decentralized [31]–[33], and hierarchical decentralized [34] fashion have been proposed; see [35] for a review. Here, we adopt the robust, decentralized algorithm proposed in [33], which relies on P, Q, V, and θ at the generators' terminal bus to estimate δ and ω. The generators are represented by the subtransient model. This model is widely accepted and not presented here because of space constraints; see, e.g., [31]. Figs. 5a and 5b (top) show δ and ω obtained from the PSS/E software, as well as their estimated values, $\hat{\delta}$ and $\hat{\omega}$.

C. Amplitude Spectrum

Fig. 5c shows that a frequency of 1.89 Hz is clearly distinguishable from the amplitude spectrum of $\hat{\delta}$. The same qualitative result is obtained for $\hat{\omega}$ in Fig. 5d. Conversely, in Figs. 5e–5h, the amplitude spectrum of variables measured by PMUs is inconclusive. The difficulties associated with estimating the modes from the signals of the bus voltage angle and frequency

TABLE II
LIST OF EIGENVALUES ASSOCIATED WITH LINEAR MODES THAT HAVE DAMPING RATIO SMALLER THAN 10%.

Mode	Freq.[Hz]	Damp.[%]	ω[rad/s]	σ[rad/s]	Mode	Freq.[Hz]	Damp. [%]	ω[rad/s]	σ[rad/s]	Mode	Freq.[Hz]	Damp. [%]	ω[rad/s]	σ[rad/s]
215	1.892	3.284	11.885	-0.391	182	0.677	7.829	4.256	-0.334	355	1.513	8.688	9.504	-0.829
260	1.957	4.077	12.294	-0.502	915	21.204	7.839	133.227	-10.476	501	2.350	8.806	14.766	-1.305
364	3.153	4.589	19.809	-0.910	636	3.721	7.861	23.378	-1.844	464	2.020	8.811	12.693	-1.123
338	2.452	4.619	15.404	-0.712	292	1.180	8.007	7.411	-0.595	488	2.209	8.957	13.882	-1.248
229	1.423	4.633	8.938	-0.415	369	1.860	8.098	11.687	-0.950	467	1.981	9.101	12.447	-1.138
283	1.867	4.861	11.732	-0.571	924	21.204	8.119	133.226	-10.852	149	0.510	9.233	3.207	-0.297
254	1.470	5.279	9.237	-0.488	925	21.204	8.119	133.226	-10.853	497	2.217	9.270	13.929	-1.297
341	2.109	5.502	13.250	-0.730	933	21.362	8.138	134.220	-10.960	602	2.801	9.448	17.598	-1.670
330	1.870	5.831	11.747	-0.686	931	21.203	8.172	133.221	-10.923	475	1.999	9.468	12.563	-1.195
336	1.843	6.063	11.583	-0.704	372	1.878	8.203	11.797	-0.971	308	1.021	9.571	6.413	-0.617
335	1.637	6.734	10.284	-0.694	331	1.326	8.215	8.330	-0.687	443	1.662	9.682	10.443	-1.016
343	1.704	6.859	10.709	-0.736	450	1.986	8.228	12.479	-1.030	357	1.399	9.687	8.791	-0.856
901	21.300	6.968	133.830	-9.348	378	1.890	8.297	11.873	-0.989	540	2.304	9.777	14.474	-1.422
301	1.361	7.094	8.552	-0.608	360	1.706	8.310	10.717	-0.894	448	1.661	9.813	10.439	-1.029
329	1.496	7.224	9.397	-0.681	896	13.824	8.391	86.856	-7.313	487	2.010	9.829	12.631	-1.248
231	0.900	7.428	5.657	-0.421	939	21.202	8.532	133.215	-11.408	710	3.441	9.831	21.620	-2.136
320	1.289	7.700	8.102	-0.626	940	21.202	8.532	133.215	-11.408	349	1.239	9.842	7.782	-0.770
362	1.862	7.726	11.702	-0.907	365	1.714	8.545	10.769	-0.924	604	2.692	9.859	16.912	-1.676
494	2.623	7.748	16.483	-1.281	379	1.843	8.560	11.582	-0.995					
916	21.353	7.792	134.166	-10.487	373	1.794	8.586	11.274	-0.972					

have also been observed by other researchers; see, e.g., [36]. One important drawback of relying on these signals for modal analysis is that they are not continuous in the strict sense. Now, discontinuities can (arguably) be removed from the signals. To this end, two approaches have been proposed in the literature:

1) *Pass the signal through a filter.* One proposal made in [37] is to remove the samples that deviate more than 3σ from the moving median of a median filter. This method suffers from two major drawbacks. First, in power systems, the standard deviations of the noise of the metering devices and their associated communications channels, including the PMUs, are estimated with large uncertainties [38]. Second, the median filter does not account for temporal correlation [39], which is precisely the case for the PMU metered values. Therefore, the simple 3σ rejection rule is not a reliable method for identifying spikes in correlated signals or time series. Similar proposals are encountered in the literature without much success; most are intrusive and inevitably modify the original signal as well as its spectrum content.

2) *Remove part of the signal containing discontinuities.* It is plausible to suppose that one could select a window of data for offline studies. The same does not apply for real-time analysis, in which case one must first be able to detect the discontinuity in the signal before removing it. There have been some attempts to detect events directly from the PMU measurements, but it is challenging to distinguish real events from measurement noises. If one could successfully detect an event from the measurements, the next step would be to remove the spike generated by that event from the signal. We did that by removing the first consecutive 25, 50, and 100 samples from the recorded data and redoing the analysis. The removal of the discontinuity led to an overall improvement of the amplitude spectrum in Figs. 5e–5h; however, the frequency of 1.89 Hz remained indistinguishable.

D. Unraveling Linear and Nonlinear Modes of Oscillation

EDMD [14] is used in this work to estimate the linear and nonlinear modes; see, e.g., [13], [14], [24] for details on the algorithm.

The results are presented in Table III. Note that three different sets of input variables are considered:

- $\hat{\delta}$ and $\hat{\omega}$

TABLE III
MODES ESTIMATED VIA EXTENDED DYNAMIC MODE DECOMPOSITION.

	$\hat{\delta}$ and $\hat{\omega}$		θ and f at Bus 6272			θ and f at Bus 6265		
Mode	Freq.[Hz]	Damp.[%]	Mode	Freq.[Hz]	Damp.[%]	Mode	Freq.[Hz]	Damp.[%]
1	3.616	1.239	1	1.569	51.737	1	1.393	69.450
2	1.822	4.615	2	10.119	76.434	2	11.177	72.062
3	5.528	5.234	3	37.149	45.397	3	60.000	28.425
4	4.963	12.061	4	60.000	30.833	4	37.836	43.057
5	0.000	100.000	5	0.000	100.000	5	0.000	100.000
6	7.991	13.472	6	0.000	100.000	6	60.000	99.515

- θ and f at Bus 6272
- θ and f at Bus 6265

and the algorithm is executed separately for each set.

We observe that the linear mode 215 with the frequency close to 1.8 Hz is captured if $\hat{\delta}$ and $\hat{\omega}$ are provided as inputs to the algorithm, and it is missed otherwise. This result is to be expected; it concurs with what was observed from the amplitude spectra in Fig. 5. Further, the second- and third-order nonlinear modes are also captured by executing the EDMD with $\hat{\delta}$ and $\hat{\omega}$, as shown by the shaded cells in Table III. For instance, we observe that mode 1 presents approximately twice the frequency of mode 2.

In summary, the discussion in this section supports to some degree the claim that DSE enhances the modal analysis of electric power grids. Further work is necessary to improve the accuracy of the EDMD in estimating the modal frequency and damping ratio, and to validate the estimated nonlinear modes. In this regard, a comparison with the *model-based* normal forms for vector fields is of interest. We are currently working along these lines, and the results will be reported elsewhere. It is remarkable that the EDMD algorithm has the potential to capture linear and nonlinear modes by using high-resolution data only, without relying on any model.

IV. CONCLUSIONS

We demonstrated through simulations, and we elaborated on the reasons why DSE is required for real-time modal analysis. Our simulations concur with the existing literature—in particular, in signal processing—as to why PMU measurements (raw sensor data) might not be a viable option for real-time stability assessments of a power system. We also illustrated how a DSE-aided, real-time dynamic stability assessment might be realized using EDMD.
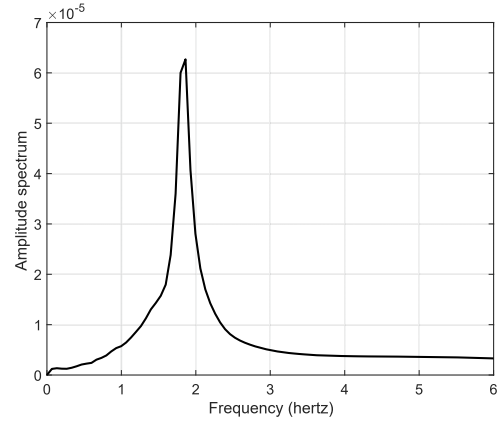
4
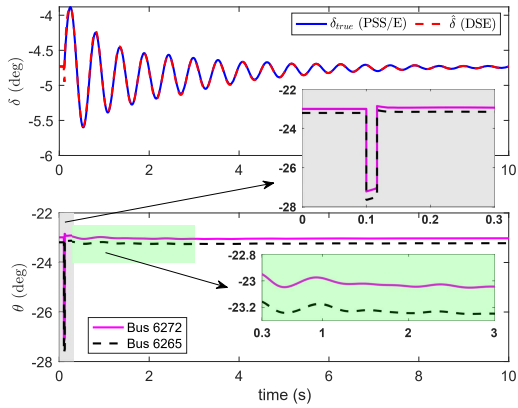
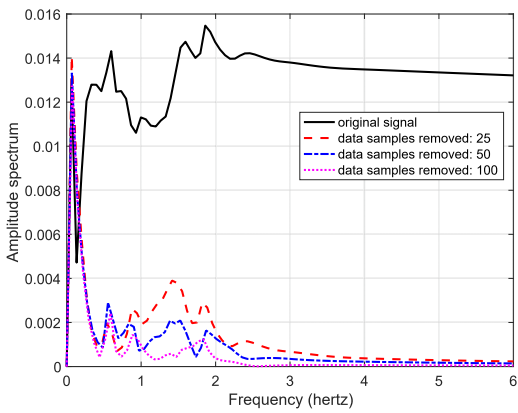(a) (top) Generator rotor angle. (bottom) Bus voltage angle.
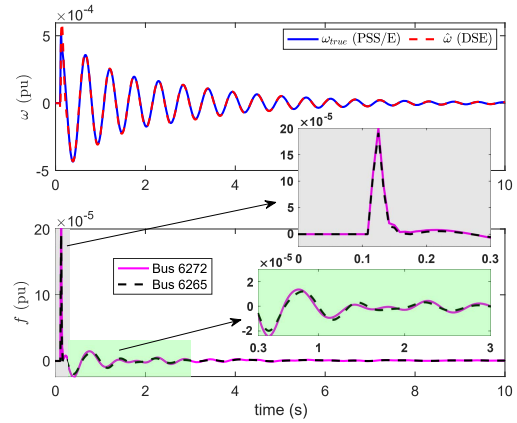
(b) (top) Generator rotor speed. (bottom) Bus frequency.
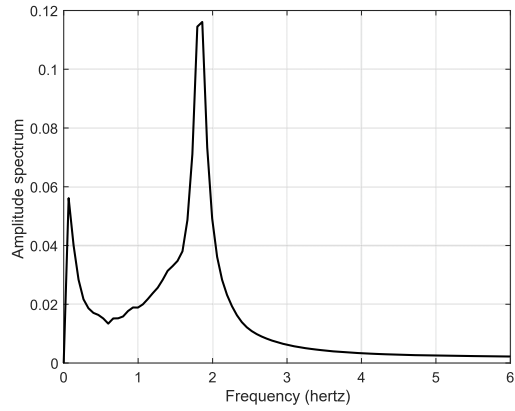
(c) Spectrum of the estimated generator rotor angle, $\hat{\delta}$.

(d) Spectrum of the estimated generator rotor speed, $\hat{\omega}$.

(e) Spectrum of voltage angle at Bus 6272.
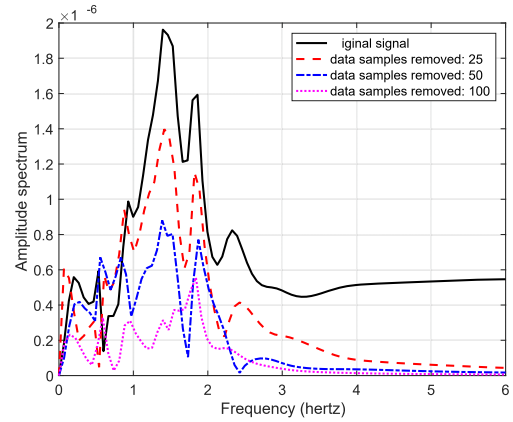
(f) Spectrum of frequency at Bus 6272.
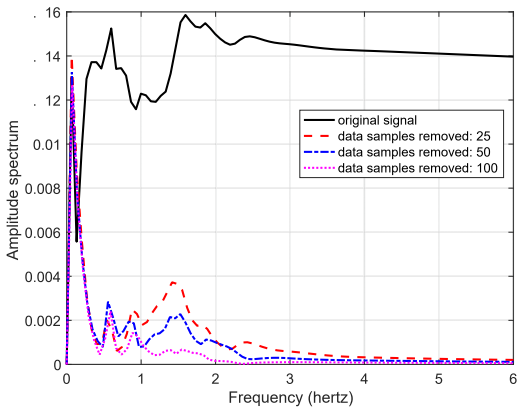
(g) Spectrum of voltage angle at Bus 6265.

(h) Spectrum of frequency at Bus 6265.

Fig. 5. Comparison between amplitude spectrum of state variables and algebraic variables. Bus 6272 is the generator terminal, and Bus 6265 is the high-voltage side of the step-up transformer connected to the same generator.

5

The capability to identify power system oscillations and the associated dynamic stability in real time will be desirable under fut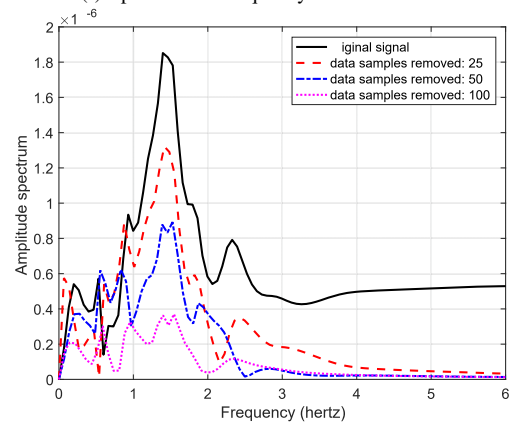ure scenarios with higher shares of power electronics-interfaced variable renewable generation. The real-time system identification and estimation capabilities will also enable time-critical control, including exploiting fast-responding power electronics converters and realizing the goals of autonomous energy grids. If poorly damped modes are detected, then appropriate controls, such as modulating power injections from converters, shall be triggered to damp them out. In alignment with this vision, the European network code already establishes that all new power plants shall be equipped with damping controls, including wind power plants. The presented research is a cog in the wheel for pushing forward the state of the art to realize such advanced, real-time system identification and control capabilities.

REFERENCES

[1] G. Rogers, "Modal analysis of power systems," *Power System Oscillations*. Springer, 2000, ch. 3, pp. 31–73.
[2] M. Netto and L. Mili, "A robust Prony method for power system electromechanical modes identification," *IEEE Power and Energy Society General Meeting (PESGM)*, July 2017, pp. 1–5.
[3] M. Netto and L. Mili, "Robust data filtering for estimating electromechanical modes of oscillation via the multichannel Prony method," *IEEE Transactions on Power Systems*, vol. 33, no. 4, 4134–4143, July 2018.
[4] L. Dosiek, N. Zhou, J. W. Pierre, Z. Huang, and D. J. Trudnowski, "Mode shape estimation algorithms under ambient conditions: A comparative review," *IEEE Transactions on Power Systems*, vol. 28, no. 2, pp. 779–787, May 2013.
[5] N. Zhou, J. W. Pierre, and J. F. Hauer, "Initial results in power system identification from injected probing signals using a subspace method," *IEEE Transactions on Power Systems*, vol. 21, no. 3, pp. 1296–1302, Aug 2006.
[6] J. C. Peng and N. C. Nair, "Enhancing Kalman filter for tracking ringdown electromechanical oscillations," *IEEE Transactions on Power Systems*, vol. 27, no. 2, pp. 1042–1050, May 2012.
[7] D. J. Trudnowski, J. W. Pierre, N. Zhou, J. F. Hauer, and M. Parashar, "Performance of three mode-meter block-processing algorithms for automated dynamic stability assessment," *IEEE Transactions on Power Systems*, vol. 23, no. 2, pp. 680–690, May 2008.
[8] F. F. Wu, K. Moslehi, and A. Bose, "Power system control centers: Past, present, and future," *Proceedings of the IEEE*, vol. 93, no. 11, pp. 1890–1908, Nov 2005.
[9] E. Barocio, B. C. Pal, N. F. Thornhill, and A. R. Messina, "A dynamic mode decomposition framework for global power system oscillation analysis," *IEEE Transactions on Power Systems*, vol. 30, no. 6, pp. 2902–2912, Nov 2015.
[10] J. Zhao, M. Netto, Z. Huang, S. Yu, A. Gómez-Expósito, S. Wang, I. Kamwa, S. Akhlaghi, L. Mili, V. Terzija, A. P. Sakis Meliopoulos, B. Pal, A. K. Singh, A. Abur, T. Bi, A. Rouhani, "Roles of Dynamic State Estimation in Power System Modeling, Monitoring and Operation," *Preprint, arXiv:2005.05380*, 2020.
[11] S. L. Marple Jr., *Digital Spectral Analysis with Applications*. Englewood Cliffs, NJ: Prentice-Hall, Inc., 1987.
[12] A. Mauroy and I. Mezić, "Global stability analysis using the eigenfunctions of the Koopman operator," *IEEE Transactions on Automatic Control*, vol. 61, no. 11, pp. 3356–3369, Nov 2016.
[13] M. O. Williams, I. G. Kevrekidis, and C. W. Rowley, "A data–driven approximation of the Koopman operator: Extending dynamic mode decomposition," *Journal of Nonlinear Science*, vol. 25, no. 6, pp. 1307–1346, Dec 2015.
[14] S. Klus, P. Koltai, and C. Schütte, "On the numerical approximation of the Perron-Frobenius and Koopman operator," *Journal of Computational Dynamics*, vol. 3, no. 1, pp. 51–79, 2016.
[15] M. Budišić, R. Mohr, and I. Mezić, "Applied Koopmanism," *Chaos: An Interdisciplinary Journal of Nonlinear Science*, vol. 22, no. 4, 2012.
[16] Y. Lan and I. Mezić, "Linearization in the large of nonlinear systems and Koopman operator spectrum," *Physica D: Nonlinear Phenomena*, vol. 242, no. 1, pp. 42 – 53, 2013.
[17] D. K. Arrowsmith and C. M. Place, *An introduction to dynamical systems*. Cambridge University Press, July 1990, ch. 2, pp. 72–79.
[18] S. K. Starrett, "Application of normal forms of vector fields to stressed power systems," Ph.D. dissertation, Iowa State University, 1994.
[19] J. J. Sanchez-Gasca, V. Vittal, M. J. Gibbard, A. R. Messina, D. J. Vowles, S. Liu, U. D. Annakkage, "Inclusion of higher order terms for small-signal (modal) analysis: committee report-task force on assessing the need to include higher order terms for small-signal (modal) analysis," *IEEE Transactions on Power Systems*, vol. 20, no. 4, pp. 1886–1904, Nov 2005.
[20] T. Tian, X. Kestelyn, O. Thomas, H. Amano, and A. R. Messina, "An accurate third-order normal form approximation for power system nonlinear analysis," *IEEE Transactions on Power Systems*, vol. 33, no. 2, pp. 2128–2139, March 2018.
[21] A. K. Singh and B. C. Pal, "Decentralized nonlinear control for power systems using normal forms and detailed models," *IEEE Transactions on Power Systems*, vol. 33, no. 2, pp. 1160–1172, March 2018.
[22] N. S. Ugwuanyi, X. Kestelyn, O. Thomas, B. Marinescu, and A. R. Messina, "A new fast track to nonlinear modal analysis of power system using normal form," *IEEE Transactions on Power Systems*, 2020.
[23] A. B. Birchfield, T. Xu, K. M. Gegner, K. S. Shetye, and T. J. Overbye, "Grid structural characteristics as validation criteria for synthetic networks," *IEEE Transactions on Power Systems*, vol. 32, no. 4, pp. 3258–3265, July 2017.
[24] M. Netto, Y. Susuki, and L. Mili, "Data-driven participation factors for nonlinear systems based on Koopman mode decomposition," *IEEE Control Systems Letters*, vol. 3, no. 1, pp. 198–203, Jan 2019.
[25] E. Ghahremani and I. Kamwa, "Dynamic state estimation in power system by applying the extended Kalman filter with unknown inputs to phasor measurements," *IEEE Transactions on Power Systems*, vol. 26, no. 4, pp. 2556–2566, Nov 2011.
[26] E. Ghahremani and I. Kamwa, "Online state estimation of a synchronous generator using unscented Kalman filter from phasor measurements units," *IEEE Transactions on Energy Conversion*, vol. 26, no. 4, pp. 1099–1108, Dec 2011.
[27] M. Netto, J. Zhao, and L. Mili, "A robust extended Kalman filter for power system dynamic state estimation using PMU measurements," *IEEE Power and Energy Society General Meeting (PESGM)*, July 2016, pp. 1–5.
[28] J. Zhao, M. Netto, and L. Mili, "A robust iterated extended Kalman filter for power system dynamic state estimation," *IEEE Transactions on Power Systems*, vol. 32, no. 4, pp. 3205–3216, July 2017.
[29] M. Netto and L. Mili, "Robust Koopman operator-based Kalman filter for power systems dynamic state estimation," *IEEE Power and Energy Society General Meeting (PESGM)*, Aug 2018, pp. 1–5.
[30] M. Netto and L. Mili, "A robust data-driven Koopman Kalman filter for power systems dynamic state estimation," *IEEE Transactions on Power Systems*, vol. 33, no. 6, pp. 7228–7237, Nov 2018.
[31] A. K. Singh and B. C. Pal, "Decentralized dynamic state estimation in power systems using unscented transformation," *IEEE Transactions on Power Systems*, vol. 29, no. 2, pp. 794–804, March 2014.
[32] E. Ghahremani and I. Kamwa, "Local and wide-area PMU-based decentralized dynamic state estimation in multi-machine power systems," *IEEE Transactions on Power Systems*, vol. 31, no. 1, pp. 547–562, 2016.
[33] J. Zhao, Z. Zheng, S. Wang, R. Huang, T. Bi, L. Mili, Z. Huang, "Correlation-aided robust decentralized dynamic state estimation of power systems with unknown control inputs," *IEEE Transactions on Power Systems*, pp. 1–1, 2019.
[34] M. Netto, V. Krishnan, L. Mili, Y. Susuki, and Y. Zhang, "A hybrid framework combining model-based and data-driven methods for hierarchical decentralized robust dynamic state estimation," *IEEE Power and Energy Society General Meeting (PESGM)*, Aug 2019, pp. 1–5.
[35] J. Zhao, A. Gómez-Expósito, M. Netto, L. Mili, A. Abur, V. Terzija, I. Kamwa, B. Pal, A. K. Singh, J. Qi, Z. Huang, A. P. Sakis Meliopoulos, "Power system dynamic state estimation: Motivations, definitions, methodologies, and future work," *IEEE Transactions on Power Systems*, vol. 34, no. 4, pp. 3188–3198, July 2019.
[36] M. Singh, A. Allen, E. Muljadi, and V. Gevorgian, "Oscillation damping: A comparison of wind and photovoltaic power plant capabilities," *IEEE Symposium on Power Electronics and Machines for Wind and Water Applications*, July 2014, pp. 1–7.
[37] L. Vanfretti, S. Bengtsson, and J. O. Gjerde, "Preprocessing synchronized phasor measurement data for spectral analysis of electromechanical oscillations in the Nordic grid," *International Transactions on Electrical Energy Systems*, vol. 25, no. 2, pp. 348–358, 2015.
[38] L. Mili, T. V. Cutsem, and M. Ribbens-Pavella, "Bad data identification methods in power system state estimation-a comparative study," *IEEE Transactions on Power Apparatus and Systems*, vol. PAS-104, no. 11, pp. 3037–3049, Nov 1985.
[39] Y. Chakhchoukh, V. Vittal, and G. T. Heydt, "PMU based state estimation by integrating correlation," *IEEE Transactions on Power Systems*, vol. 29, no. 2, pp. 617–626, March 2014.